Arch. Immunol. Ther. Exp. (2017) 65:241–252
DOI 10.1007/s00005-016-0424-8

ORIGINAL ARTICLE

A Quinone-Containing Compound Enhances Camptothecin-Induced Apoptosis of Lung Cancer Through Modulating Endogenous ROS and ERK Signaling

Han-Lin Chou[1,2] · Yao Fong[3] · Chi-Ku Wei[1] · Eing-Mei Tsai[4] · Jeff Yi-Fu Chen[1] · Wen-Tsan Chang[5,6] · Chang-Yi Wu[1,7] · Hurng-Wern Huang[2] · Chien-Chih Chiu[1,4,7,8]

Received: 18 January 2016 / Accepted: 21 July 2016 / Published online: 27 September 2016

Abstract The natural compound camptothecin (CPT) derivatives have widely been used for anti-cancer treatments, including lung cancer. However, many chemoresistant cancer cells often develop a relatively higher threshold for inducing apoptosis, causing a limited efficacy of anti-cancer drugs. Likewise, lung cancer cells acquire chemoresistance against CPT analogs, such as irinotecan and topotecan, finally resulting in an unsatisfied outcome and poor prognosis of lung cancer patients. TFPP is a quinone-containing compound as a candidate for CPT-based combination chemotherapy. In this study, we examined the effect of TFPP and CPT cotreatment on non-small cell lung cancer (NSCLC) cells. Cell proliferation and flow cytometry-based Annexin-V/PI staining assays demonstrated the synergistic effect of TFPP on CPT-induced apoptosis in both NSCLC A549 and H1299 cells. The results of CPT and TFPP cotreatment cause the regulation of the ERK-Bim axis and the activation of mitochondrial-mediated caspase cascade, including caspase-9 and caspase-3. Besides, TFPP significantly enhanced CPT-induced endogenous reactive oxygen species (ROS) in the two NSCLC cells. In contrast, the treatment of N-acetyl-L-cysteine (NAC), an ROS scavenger, rescues the apoptosis of NSCLC cells induced by TFPP and CPT cotreatment, suggesting that the synergistic effect of TFPP on CPT-induced anti-NSCLC cells is through upregulating ROS production. Consequently, our results suggest that TFPP sensitizes NSCLC towards CPT-based chemotherapy may act through decreasing the apoptosis-initiating threshold. Therefore, TFPP may be a promising chemosensitizer for lung cancer treatment, and the underlying mechanism warrants further.

Keywords Non-small cell lung cancer · Chemoresistance · Apoptosis threshold · Camptothecin · TFPP · ERK signaling pathway

Electronic supplementary material The online version of this article (doi:10.1007/s00005-016-0424-8) contains supplementary material, which is available to authorized users.

✉ Hurng-Wern Huang
sting@mail.nsysu.edu.tw

✉ Chien-Chih Chiu
cchiu@kmu.edu.tw

[1] Department of Biotechnology, Kaohsiung Medical University, Kaohsiung 807, Taiwan

[2] Institute of Biomedical Science, National Sun Yat-Sen University, Kaohsiung 80424, Taiwan

[3] Department of Thoracic Surgery, Chi-Mei Medical Center, Tainan 710, Taiwan

[4] Research Center for Environment Medicine, Kaohsiung Medical University, Kaohsiung 807, Taiwan

[5] Division of Hepatobiliary and Pancreatic Surgery, Department of Surgery, Kaohsiung Medical University Hospital, Kaohsiung 807, Taiwan

[6] Department of Surgery, School of Medicine, College of Medicine, Kaohsiung Medical University, Kaohsiung 807, Taiwan

[7] Department of Biological Sciences, National Sun Yat-Sen University, Kaohsiung 804, Taiwan

[8] The Graduate Institute of Medicine, Kaohsiung Medical University, Kaohsiung 807, Taiwan

Introduction

Lung cancer is the most common cause of cancer death worldwide. Non-small cell lung cancer (NSCLC) accounts for about 80 % of lung cancer. Chemotherapeutic agents have provided the standard regimens backbone for resected lung cancer patients as combination chemotherapy (Strauss et al. 2008). For example, high dose of platinum-based agents, such as cisplatin and carboplatin, or camptothecin (CPT) derivative-based agents, such as irinotecan and topotecan, are widely used for NSCLC treatments (Cimino et al. 2013). However, resistance to adjuvant systemic chemotherapy is a common phenomenon in NSCLC patients, causing poor prognosis and recurrence (Tamburini et al. 2000). Therefore, an improved efficacy of adjuvant chemotherapeutic agent for NSCLC patients has still been developing.

The locations of distant tumor recurrence for NSCLC patients are most commonly seen (Hung et al. 2012). The risk of distant tumor recurrence for NSCLC patients has been reduced by adjuvant combination chemotherapy. The adjuvant combination chemotherapy, an additional treatment with other anti-cancer drugs, has been reported to greatly improve the overall survival of stage I-IIIA NSCLC patients (Liang and Wakelee 2013). For example, the combination of irinotecan/cisplatin or carboplatin and topotecan/carboplatin has reported to enhance the overall survival for NSCLC patients (Kim et al. 2006; Patel et al. 2007; Read et al. 2004). Therefore, the optimization of the efficiency and cytotoxicity of adjuvant combination chemotherapy still represents an important issue in cancer treatment.

CPT, a pentacyclic quinoline plant alkaloid, was reported to exhibit various bioactivities, including anti-cancer activity (Zeng et al. 2012). CPT derivatives, such as irinotecan and topotecan, were widely used anti-cancer drugs against multiple cancers, including lung cancer (Yang et al. 2015). However, treatment of irinotecan or topotecan-induced chemoresistance limited anti-cancer effects in NSCLC patients (Westover et al. 2015). Therefore, to reduce the acquired chemoresistance of NSCLC patients, these drugs are widely used in combination with other adjuvant chemotherapy. For example, there is increased anti-lung cancer activity of CPT and its derivatives in cotreatment with other anti-lung cancer agents, such as irinotecan/doxorubicin (Xenidis et al. 2011) and topotecan/cisplatin (Ichinose et al. 2011).

Quinone-containing compounds were reported to exert various bioactivities, including anti-fungal, anti-protozoal, anti-bacterial, and anti-cancer activity (Benites et al. 2008). Quinone compounds have been shown to exert the anti-cancer activity by modulating endogenous ROS. For instance, doxorubicin, a quinone compound, has been shown to induce the apoptosis of osteosarcoma Saos-2 cells through inducing ROS (Tsang et al. 2003). On the other hand, the combinations of quinone-containing compounds and other chemotherapeutic agents were reported to treat various cancer cells. For instance, the combination of doxorubicin and topotecan synergistically inhibits cell growth of ovarian cancer SKOV-3 cells (Patankar et al. 2013). Likewise, mitomycin C, a quinone compound isolated from *Streptomyces caespitosus,* was applied in combination with irinotecan, potentially inhibiting gastric cancer in phase II clinical trial study (Ogawa et al. 2012). These reports suggest that quinone-containing compounds could be a potential adjuvant agent for synergistically enhancing the CPT analogs-induced anti-cancer effects. Therefore, we screened for effective quinone-containing compounds to optimize the inhibition of cell growth and induction of apoptosis in NSCLC cells.

To overcome the limitations of CPT-based treatment against NSCLC, a quinone-containing compound, 4-[2356-tetrafluoro-4-(4-hydroxyphenoxy)phenoxy]phenol (TFPP), was identified. In this study, we investigated the synergistic effect and the mechanism of TFPP on CPT-induced apoptosis of NSCLC. Furthermore, the modulation of endogenous reactive oxygen species (ROS) and the role of mitogen-activated protein kinases (MAPK) extracellular signal-regulated kinase (ERK) in NSCLC cells following CPT and TFPP cotreatment were discussed.

Materials and Methods

Preparation of TFPP and CPT

TFPP was purchased from the chemical supplier Enamine^{TM} (Kiev, Ukraine). CPT was purchased from Sigma-Aldrich (St. Louis, MO, USA). Both TFPP and CPT were dissolved in DMSO (below 0.01 %) immediately prior to assays.

Reagents

Antibiotics penicillin G and streptomycin, DMEM medium, and fetal bovine serum (FBS) were purchased from Gibco BRL (Gaithersburg, MD, USA). Trypan blue, Dimethyl sulphoxide (DMSO), and ribonuclease A (RNase A) were purchased from Sigma-Aldrich (St. Louis, MO, USA). Antibodies against phospho-ERK (Thr^{202}/Tyr^{204}) (#9101), total-ERK (#9102), cleaved caspase-9 (#7237), and cleaved caspase-3 (#9961) were purchased from Cell signaling technology (San Jose, CA, USA). Antibody against glyceraldehyde 3-phosphate dehydrogenase

(GAPDH) was obtained from Santa Cruz Biotechnology (Santa Cruz, CA, USA). Both anti-mouse and anti-rabbit IgG peroxidase-conjugated secondary antibodies were purchased from Leadgene Biomedical (#20102 and #20202, respectively, Tainan, Taiwan). Annexin-V-Fluorescein isothiocyanate (FITC) detection kit was purchased from Strong Biotech Co. (Taipei, Taiwan).

Cell Culture

Human NSCLC cells A549 and H1299 were obtained from the American Type Culture Collection (ATCC; Manassas, VA, USA). Cells were incubated in DMEM: F-12 (3:2) with 8 % FBS, 100 units/ml penicillin and 100 μg/ml streptomycin, and 2 mM glutamine at 37 °C in a humidified atmosphere of 5 % CO_2. Cells were tested using a PCR-based assay described previously to ensure the free of mycoplasma contamination with minor modifications (Wirth et al. 1994).

Proliferative Inhibition Assay

The cellular viability and proliferation rate were determined by the Trypan blue dye exclusion assay. Briefly, 3×10^4 NSCLC A549 and H1299 cells were seeded and treated with DMSO with vehicle or the indicated concentrations of CPT and TFPP alone, or cotreatment for 24 and 48 h. After incubation, cells were stained with 0.2 % Trypan blue and counted by Countess™, an automatic cell counter (Invitrogen).

Colony Formation Assay

We performed the colony formation assay to confirm the anti-cell proliferative potential of TFPP as described previously with minor modifications (Fong et al. 2014). In brief, 4×10^2 of two NSCLC cell lines A549 and H1299 were seeded into a six-well plate and treated with indicated concentrations of CPT and TFPP alone or in combination for 48 h, respectively. After incubation of 11 days, colonies were paraformaldehyde-fixed and Giemsa-stained. The area of colonies was analyzed by the software Image-Pro Plus (Media Cybernetics; MA, USA).

Assessment of Drug Synergism

The values of combination index were analyzed by the CalcuSyn software based on the Chou–Talalay method (Biosoft, Cambridge, UK) (Chou and Talalay 1981, 1984). The 95 % confidence intervals for the values of dose–response were assessed for determining the synergism of TFPP and CPT combination.

Apoptosis Assessment

To examine the apoptosis-inducing potential of CPT and TFPP alone, or cotreatment, Annexin-V/PI double staining was performed to detect the externalization of phosphatidylserine from the plasma membrane. In brief, 1×10^5 cells were seeded onto a six-well plate and treated with CPT and TFPP alone, or cotreatment for 24 and 48 h, respectively. Subsequently, cells were harvested and stained with Annexin-V/PI, and cells were analyzed by the flow cytometer (Accuri C6; BD Biosciences, San Jose, CA, USA).

Oxidative Stress Assessment

Intracellular redox state was determined by the ROS-sensitive fluorescence dyes dihydroethidium (DHE; Merck, Darmstadt, Germany) and MitoSox (Invitrogen, Carlsbad, CA, USA). In brief, 1×10^5 cells of NSCLC cell lines A549 and H1299 were seeded into a six-well plate and treated with 0.5 μM CPT and 10 μM TFPP alone, or cotreatment for 6 h, respectively. Subsequently, cells were incubated with the medium in the presence of either 1 μM DHE or 5 μM MitoSox at 37 °C for 30 min in darkness, respectively. After incubation, cells were harvested, thoroughly washed, and resuspended in 0.2 ml PBS. Finally, cells were analyzed by a flow cytometry (Muse™ Cell Analyser, Merck Millipore, Billerica, MA, USA). The wavelength of excitation for oxidation of DHE and MitoSox was excited at 510 nm, and the wavelengths of emission were at 580 nm (DHE) and 610 nm (MitoSox), respectively.

Western Blot Analysis

Western blotting was performed as previously described (Chiu et al. 2015). Briefly, cells were harvested and lysed. The protein concentration was determined. 20 μg protein was loaded and resolved by 10 % SDS-polyacrylamide gel electrophoresis and then was electrotransferred to a PVDF membrane. The membrane was blocked and incubated with primary and secondary antibodies against specific proteins. The signals were detected using an enhanced chemiluminescence detection kit (Advansta Corp., Menlo Park, CA, USA).

Assessment of ERK Inhibition

To further determine the role of ERK in CPT and TFPP combination-induced anti-NSCLC effect, a total of 1×10^5 cells were seeded into a six-well plate and were pre-treated for 3 h with ERK-specific inhibitor PD98059

(Enzo Life Sciences Inc., NY, USA) before CPT and TFPP combination. Afterward, the long-term proliferation and apoptosis of NSCLC cells were analyzed using the colony formation assay and Annexin-V/PI double staining assay, respectively.

Caspase Inhibition Assay

1×10^5 cells were seeded and pre-treated with caspase-specific inhibitors Z-IETD-FMK (#075C, G-Biosciences, St. Louis, MO, USA) for caspase-8 and Z-LEHD-FMK for caspase-9 (#CPI-009, G-Biosciences) for 3 h, respectively, and then, the cells were subject to the treatment of CPT and TFPP combination for 48 h. Subsequently, the cells were harvested and detected by the flow cytometer-based Annexin-V/PI assay.

Statistical Analysis

Differences between the combination of CPT with TFPP and CPT-treated cells were analyzed in at least triplicate experiments. The differences were analyzed by the one-way analysis of variance (ANOVA), with $p < 0.05$ was statistically significant.

Results

CPT and TFPP Cotreatment Exerts an Enhanced Anti-Lung Cancer Potential

We first examined the synergistic effects of TFPP on CPT-induced anti-proliferation of NSCLC H1299 cells using the Chou–Talalay method (Chou and Talalay 1981, 1984). The results were calculated using the software CalcuSyn, in which CPT's EC_{50} value was 0.5 μM for cell proliferation in H1299 cells (Supplementary Fig. 1). Compared with CPT treatment alone, the combination of CPT and TFPP synergistically inhibited cell proliferation of H1299 cells. To further evaluate the effect of CPT and TFPP cotreatment on cell growth of NSCLC cells, the survival rate of two NSCLC A549 and H1299 cells was determined by Trypan blue exclusion assay. As shown in Fig. 1a, b, either CPT or TFPP alone exhibited none or low cytotoxicity toward NSCLC A549 and H1299 cells. However, the cell survival rate significantly reduced to approximately 70 % and 85 % after the cotreatment of CPT and TFPP for 24 and 48 h, respectively. Consistently, colony formation assay showed that CPT and TFPP cotreatment significantly inhibited the long-term proliferation of two NSCLC cells (Fig. 1c, d). These results suggest that the combination of TFPP and CPT synergistically inhibits the growth of NSCLC cells.

TFPP Enhances CPT-Induced Apoptosis

To determine whether the combination of TFPP and CPT inhibits cell survival by inducing apoptosis, flow cytometry-based assay was performed using Annexin-V/PI dual staining. The percentages of Annexin-V-positive/PI-negative and Annexin-V-positive/PI-positive represent early and late-apoptosis, respectively. After CPT cotreatment with TFPP, the proportion of apoptotic cells significantly increased in two NSCLC cells in a time-response manner (Fig. 2). These results showed that TFPP synergistically enhances CPT-induced apoptosis of two NSCLC cells.

The Role of MAPK in CPT/TFPP Combination-Induced Inhibitory Effect on Colony Formation of NSCLC Cells

MAPKs are critical for the maintenance of cellular proliferation and apoptosis (Coulthard et al. 2009; Michaelidis et al. 2009). Furthermore, the involvement of MAPKs in anti-cancer drug-induced apoptosis has been documented (Chen et al. 2015; Ong et al. 2015).

Therefore, to examine whether MAPK members play a role in CPT and TFPP combination-induced anti-NSCLC effect, colony formation in the presence of MAPK inhibitors, including JNK (SP600125), p38 MAPK (SB203580), and ERK (PD98059), was evaluated. As shown in Fig. 3, the results showed that ERK blockage significantly reduces the colony formation of both two NSCLC cell lines, suggesting the pro-survival role of ERK in CPT and TFPP cotreatment-induced anti-proliferation of NSCLC cells.

TFPP Enhances CPT-Induced Endogenous ROS Production

ROS has been shown to play a critical role in regulating the apoptosis of tumor cells (Jayasooriya et al. 2014). Next, we determined whether the relative levels of ROS production in NSCLC cells treated with CPT were affected by TFPP. As shown in Fig. 3, the relative levels of ROS production were measured using DHE staining coupled with a flow cytometry. The results revealed that TFPP treatment markedly enhances CPT-induced ROS production in NSCLC cells, compared with those treated with CPT or TFPP alone (Fig. 4).

NAC Reduces Endogenous ROS in CPT/TFPP-Treated NSCLC Cells

MitoSox™ Red, a DHE derivative, conjugates to lipophilic and positively charged triphenylphosphonium, selectively detecting superoxide (O_2^-) in the mitochondria of a living cell. Therefore, we used MitoSox fluorescence dye to

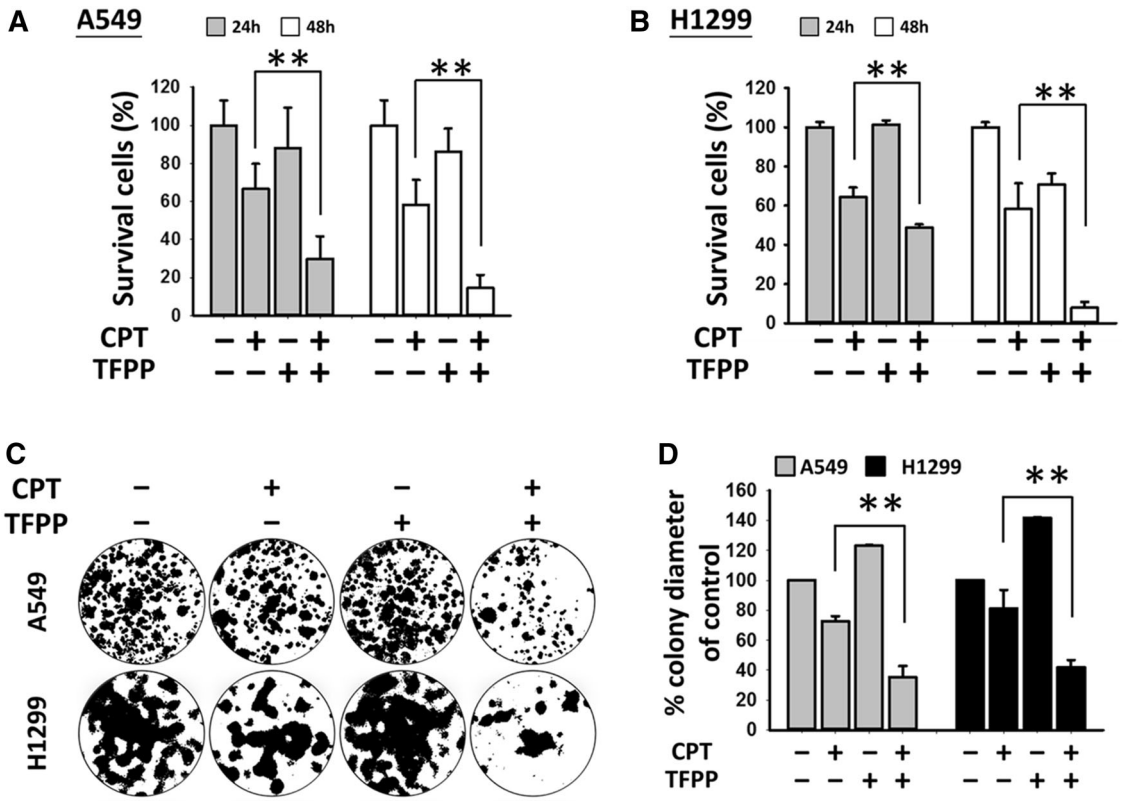

Fig. 1 TFPP sensitizes two NSCLC cells to CPT-induced anti-proliferation of NSCLC cells. **a** A549 and **b** H1299 cells were incubated with 0.5 μM CPT, 10 μM TFPP alone, or the combination of CPT and TFPP, respectively. The rates of cell survival were determined using the Trypan blue exclusion assay (**$p < 0.001$, $n = 3$). **c** The long-term effect of CPT and TFPP combination on the proliferation was determined using a colony formation assay. NSCLC cell lines A549 and H1299 were seeded and incubated with indicated treatments. The cells were fixed and Giemsa-stained. **d** The quantificative result of the colony formation. Data are presented as mean ± SD

examine if mitochondria are the primary source of ROS production following CPT treatment. The results showed that the scavenger of ROS by *N*-acetyl-L-cysteine (NAC) decreases the fluorescence intensity of MitoSox in CPT-treated NSCLC cell, whereas the blockage of ERK did not affect CPT-induced ROS production from mitochondria (Supplementary Fig. 2). The above results suggest that mitochondria should be the primary source of ROS production in CPT-treated NSCLC cells.

Next, we examined whether the ROS production is involved in treating efficacy of CPT and TFPP cotreatment. As shown in Fig. 5, NAC, a potent ROS scavenger significantly reduced the ROS production of two NSCLC cells treated with CPT alone or the cotreatment, suggesting that the combination of TFPP and CPT synergistically increases the generation of ROS in cells.

ROS Scavenger Attenuates CPT/TFPP-Induced Apoptosis of Lung Cancer Cell

To determine whether the reduction of ROS production affects apoptosis of NSCLC cells, we evaluated whether CPT and TFPP cotreatment-induced apoptosis was mediated via ROS production. NSCLC cells were pre-treated with or without 2 mM NAC for 3 h, followed by the cotreatment of CPT and TFPP for 6 h, respectively. Our results showed that pre-treatment of NAC significantly reduced CPT/TFPP-induced apoptosis of two NSCLC cells (Fig. 6), suggesting that CPT and TFPP cotreatment sensitizes lung cancer cells toward apoptosis through regulating ROS production.

The Regulation of ERK Phosphorylation and Caspase Activation in Lung Cancer Cells Following TFPP and CPT Combination

To further explore the mechanism by which TFPP increases CPT-induced apoptosis of lung cancer cells, we investigated whether TFPP could promote CPT-induced apoptosis. We examined whether TFPP treatment affects the activation of caspase-9 and caspase-3 in NSCLC A549 cells. As shown in Fig. 7a, CPT and TFPP cotreatment synergistically enhances the proteolytic activation of caspase-9 and caspase-3 in NSCLC A549

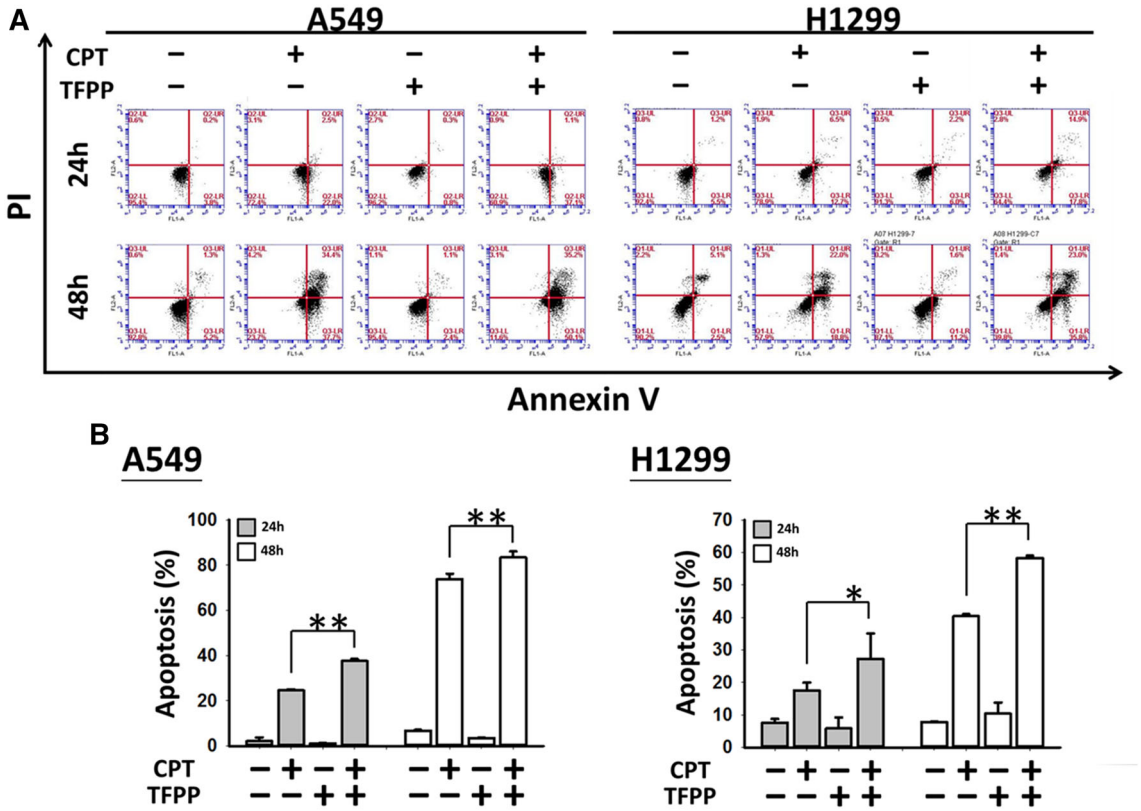

Fig. 2 TFPP significantly enhances CPT-induced apoptosis of two NSCLC cells. **a** Two NSCLC cells were treated with 0.5 μM CPT alone, 10 μM TFPP alone or in combination with CPT/TFPP for 24 and 48 h, respectively. Apoptotic percentages were stained with the Annexin-V/PI double staining analysis. **b** The quantitative analysis of apoptotic cells. The statistical significance between TFPP/CPT cotreatment and CPT treatment alone ($*p < 0.05$, $**p < 0.001$; $n = 3$)

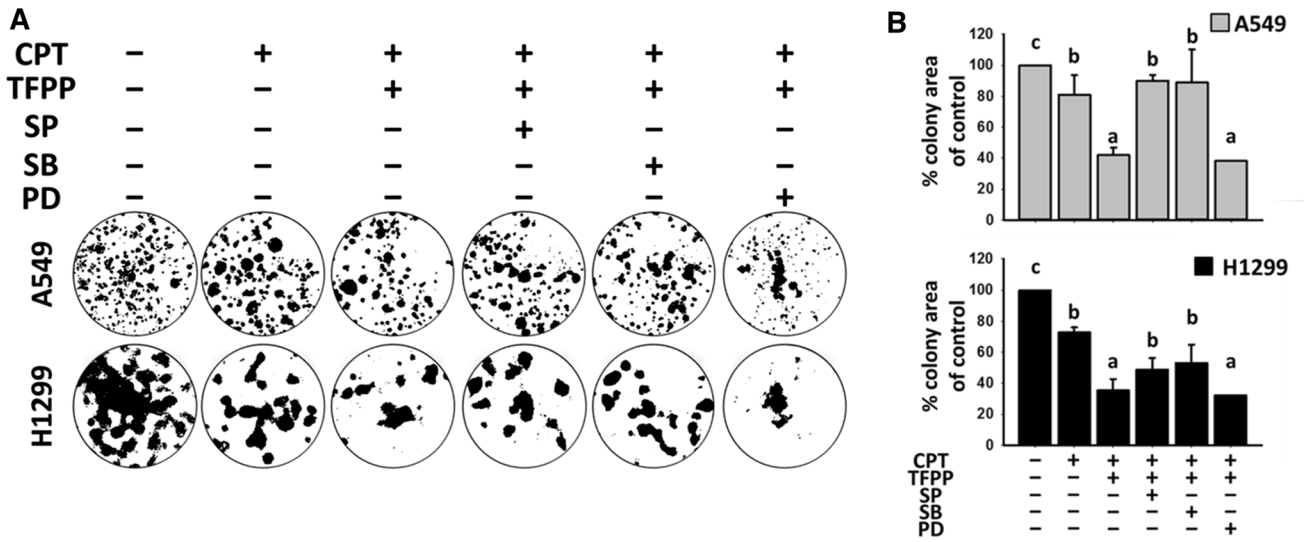

Fig. 3 Role of MAPK in CPT and TFPP combination-induced long-term anti-proliferation. Two NSCLC cell lines A549 and H1299 were seeded and pre-treated with MAPK inhibitor JNK (SP600125, 10 μM), p38 (SB203580, 10 μM), and ERK (PD98059, 10 μM) for 3 h, and then were subject to indicated treatments, respectively. **a** Afterward, cells were paraformaldehyde-fixed and Giemsa-stained. **b** The quantitative analysis of the colony area. Data are presented as mean ± SD ([a]not statistical significance; [b]$p < 0.05$; [c]$p < 0.001$)

cells. We found that TFPP significant decreases CPT-induced the expression of phosphor-ERK (Thr^{202}/Tyr^{204}) in NSCLC A549 cells. Besides, CPT and TFPP cotreatment enhances Bim upregulation, which is a downstream target of ERK signaling pathway. These results suggest that CPT and TFPP cotreatment enhances

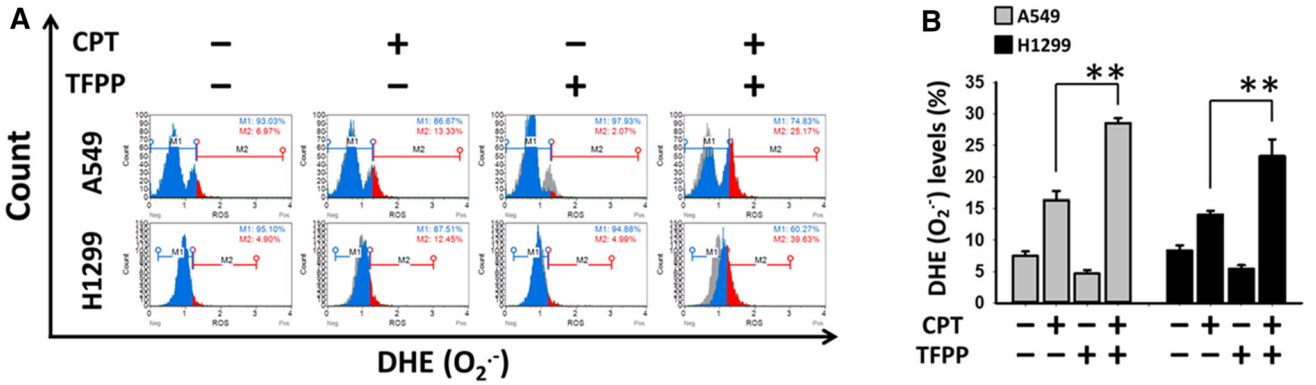

Fig. 4 TFPP synergistically increases CPT-induced ROS production in NSCLC cells. **a** NSCLC cells were treated with 0.5 μM CPT alone and 10 μM TFPP alone or in combination with CPT/TFPP for 6 h. The levels of ROS production were determined by DHE staining and then flow cytometry analysis at 6 h after cotreatment of CPT and TFPP. **b** The relative levels of ROS production in A549 and H1299 cells cotreated with CPT and TFPP compared with CPT treatment alone (**$p < 0.001$)

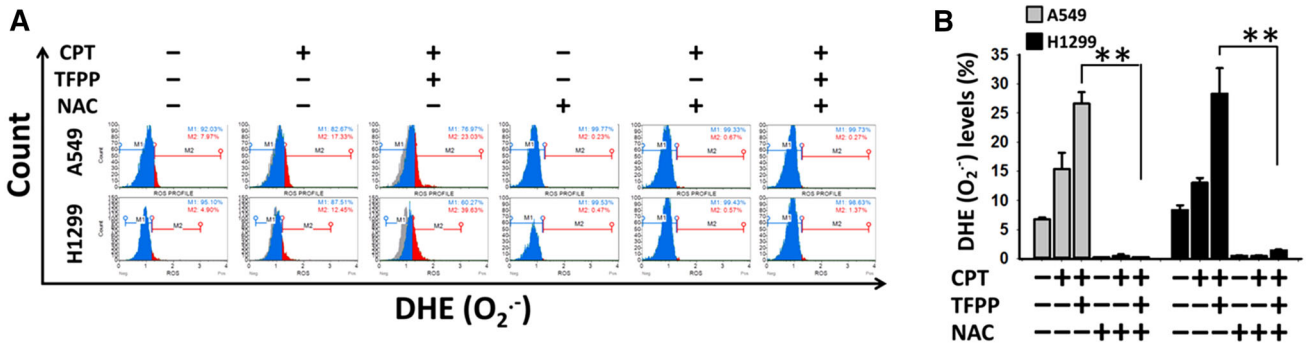

Fig. 5 Pretreatment with NAC attenuates CPT/TFPP-induced ROS production in NSCLC cells. **a** A549 and H1299 cells were pre-treated with 2 mM NAC for 3 h and were then treated with CPT (0.5 μM), or CPT/TFPP cotreatment for 6 h, respectively. The production of ROS was quantified using the flow cytometry-based DHE staining assay. **b** The relative levels of ROS production in treated groups with NAC pre-treatment (**$p < 0.001$)

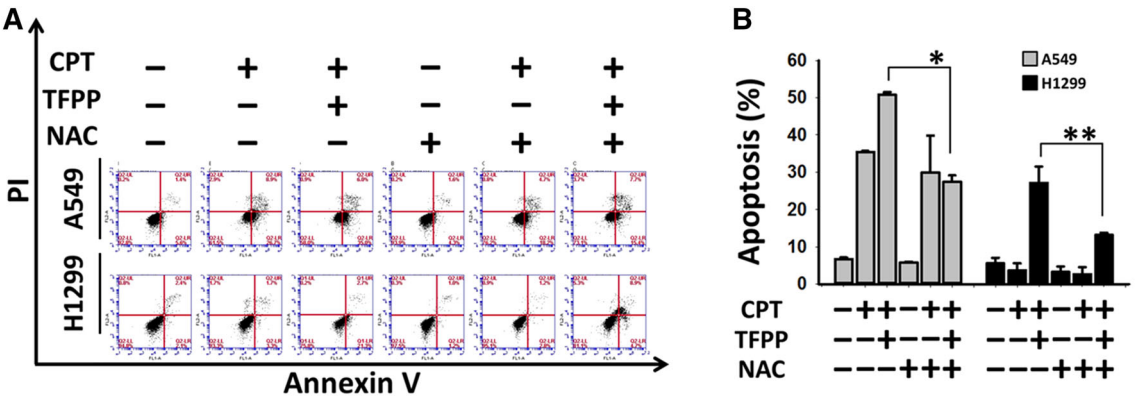

Fig. 6 ROS scavenger reduces CPT/TFPP-induced apoptosis of NSCLC cells. **a** A549 and H1299 cells were pre-treated with 2 mM NAC for 3 h, respectively, then subject to cotreatment of 0.5 μM CPT and 10 μM TFPP for 24 h which was described in "Materials and Methods" section. **b** The quantitative analysis of **a**. *Different letter* notations indicate the statistical significance between CPT/TFPP cotreatment with or without NAC (*$p < 0.05$, **$p < 0.001$)

the apoptosis of A549 cells through regulating ERK activation.

The initiation of apoptosis triggered by two major pathways: the extrinsic- (death receptor-mediated) and the intrinsic (mitochondria-mediated)-pathways (Tait and Green 2010). Therefore, we sought to determine which apoptosis pathway mediates CPT and TFPP cotreatment-induced apoptosis of NSCLC cells. As shown in Fig. 7b,

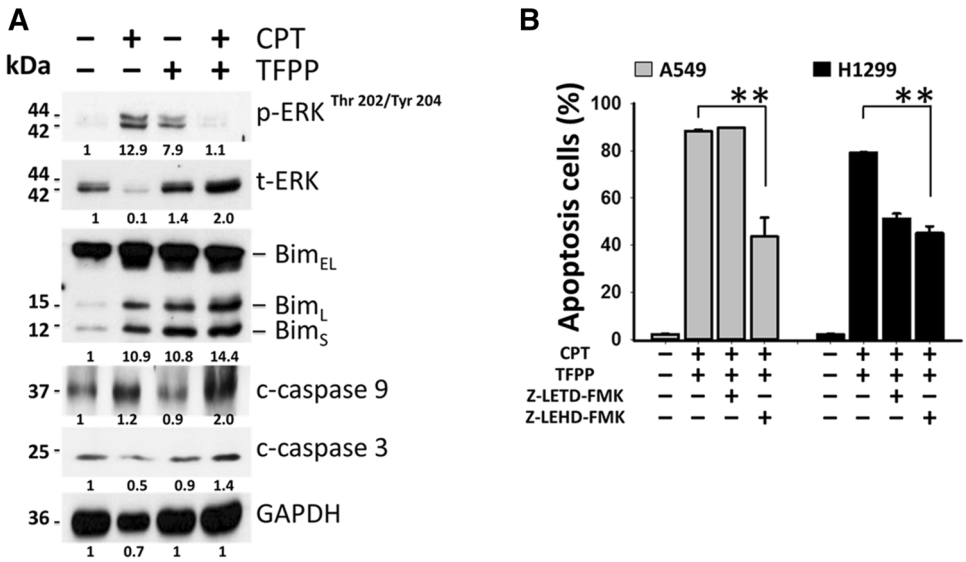

Fig. 7 CPT and TFPP cotreatment induces pro-apoptotic proteins through inhibiting ERK activation. **a** A549 cells were subjected to treatment with vehicle control or the indicated doses of CPT and TFPP alone, or cotreatment. Western blot showed the significantly decreased levels of phosphorylation of ERK (Thr^{202}/Tyr^{204}), whereas increased the protein level of pro-apoptotic Bim. *p-ERK* ERK, *t-ERK* total-ERK, *c-caspase-9* cleaved caspase-9, *c-caspase-3* cleaved caspase-3. GAPDH was measured as an internal control. Each blot is representative of at least three independent experiments. **b** The quantificative analysis of caspase inhibitor assay. Two NSCLC cell lines A549 and H1299 were pre-treated with caspase inhibitors against caspase-9 (Z-LETD-FMK) and caspase-8 (Z-LEHD-FMK) for 3 h, respectively, and then, cells were subject to TFPP in combination with CPT for 48 h. Cells were stained with Annexin-V assay for detecting apoptosis. Data are presented as mean ± SD (**$p < 0.001$)

Annexin-V-staining showed that the inhibition of caspase-9 by Z-LEHD-FMK, the marker of intrinsic apoptosis pathway, significantly attenuated the combination of CPT and TFPP-induced apoptosis of two NSCLC cell lines, whereas the inhibition of caspase-8 by Z-IETD-FMK, the marker of death receptor-mediated apoptosis pathway, did not affect apoptosis of NSCLC cells.

ERK Blockade Enhances CPT/TFPP-Induced Apoptotic Lung Cancer Cells

To confirm CPT/TFPP-induced suppression of ERK activation in both A549 and H1299 cells, we further examined whether blockage of ERK activation enhances CPT/TFPP-induced apoptosis in lung cancer cells. As shown in Fig. 8, we found that blockade of ERK activation partially increased the number of apoptotic NSCLC cells after CPT and TFPP cotreatment. These results indicate that the pro-survival role of ERK is moderately involved in CPT-induced apoptotic cell death.

Discussion

Currently, chemotherapeutic agents in combination with other anti-cancer drugs have been significantly improved survival of NSCLC patients as adjuvant combination chemotherapy. Adjuvant combination chemotherapies, including platinum-based or CPT derivatives-based chemotherapy, have been reported to prolong the survival rate of advanced NSCLC patients (Cimino et al. 2013). However, the recurrence rate for NSCLC patients with post-resection is still up to 50 % (Uramoto and Tanaka 2014). Furthermore, the development of chemoresistance is highly correlated with the high recurrence and poor prognosis of NSCLC patients (Gallego et al. 2008).

Higher level of endogenous ROS, a known intracellular second messenger, has been detected in many chemoresistant cancer cells (Mor et al. 2008). Furthermore, chemoresistant cancer was also found to have a higher threshold of apoptosis induced by anti-cancer drugs (Fraser et al. 2003; Mor et al. 2008). For instance, gefitinib, a tyrosine kinase inhibitor, was widely used as a clinically chemotherapeutics in human lung cancer. However, the previous study showed that lung cancer H460 cells acquire gefitinib resistance through increasing the threshold of ROS-induced apoptosis (Okon et al. 2015). Therefore, sensitizing cancer cells toward chemotherapy by reducing the apoptotic threshold, it appears to be a promising strategy (Barrera 2012; Wang and Yi 2008). For example, Wang and Yuan (2013) found that gambogic acid, a proteasome inhibitor, derived from Chinese herbs, sensitizes doxorubicin-resistant ovarian cancer SKOV-3 cells to the drug through lowering the threshold of ROS-induced apoptosis.

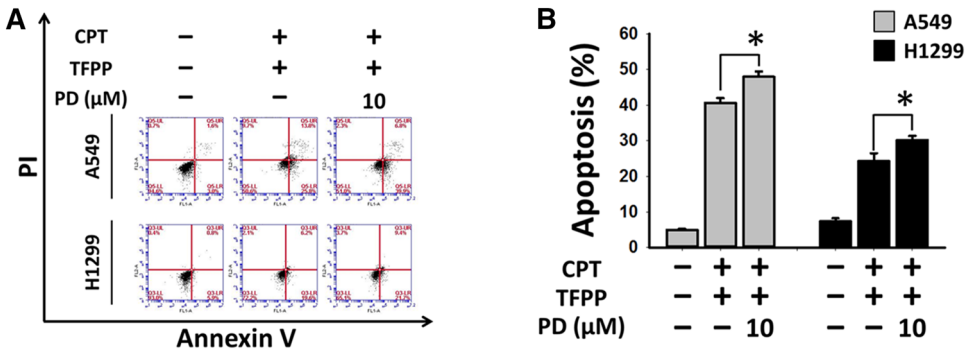

Fig. 8 Blockage of ERK activation enhances CPT/TFPP-induced apoptosis of both A549 and H1299 cells. **a** Effect of ERK suppression on CPT/TFPP-induced apoptosis of both A549 and H1299 cells determined using a flow cytometry-based Annexin-V/PI staining assay. **b** Quantitative analysis of apoptotic cells. Different letter notations indicate the statistical significance between combination of CPT and TFPP with or without ERK inhibitor (PD98059) (*$p < 0.05$)

Quinone-containing compounds have been shown to modulate the production of ROS, including superoxide, hydrogen peroxide, and hydroxyl radical (Bolton et al. 2000). For example, two known quinones doxorubicin and mitomycin C exhibit anti-cancer effects through regulating the generation of ROS (Sharma et al. 2007; Shi et al. 2013). In comparison with doxorubicin and mitomycin C, TFPP has the potential to induce the production of endogenous ROS without a significant cytotoxicity. In addition, the low cytotoxicity of TFPP may also reduce the toxic side effects of combination chemotherapy. Therefore, TFPP may be a promising chemosensitizer by lowering the threshold of ROS-mediated apoptosis. Accordingly, we examined whether TFPP could exert an effect on CPT-induced anti-proliferation of NSCLC cells. The results showed the synergistic effect of TFPP on CPT-induced anti-proliferation and apoptosis of NSCLC cells (Figs. 1, 2). These findings suggest that TFPP may be a promising adjuvant to CPT-based lung cancer therapy in the future.

MAPK pathways are important for regulating growth, survival, and death in cells (Coulthard et al. 2009; Michaelidis et al. 2009). Furthermore, many anti-cancer drugs have reported stimulating MAPK-mediated apoptosis of cancer cells, including lung cancer (Ong et al. 2015) and colorectal carcinoma cells (Chen et al. 2015). Our results showed that the blockage of ERK by specific inhibitors significantly reduced cell proliferation in both A549 and H1299 cells treated with CPT and TFPP (Fig. 3), suggesting the pro-survival role of ERK in CPT/TFPP-cotreated NSCLC cells.

The previous study suggested that cancer cells could acquire chemoresistance by increasing ROS-induced apoptotic threshold (Wang et al. 1999). Moreover, these chemoresistant cancer cells seem to be tolerant to increased endogenous ROS by upregulating antioxidant capacity (Trachootham et al. 2009). Furthermore, moderate increase of ROS promotes proliferation and survival of the chemoresistant cancer cells (Trachootham et al. 2008). Therefore, exogenous ROS-generating agents or compounds sensitize cancer cells toward the elevation of oxidative stress through overwhelming the antioxidant capacity. Therefore, a possible anti-cancer strategy is to elevate the oxidative stress while lowering ROS-induced apoptosis threshold, eventually leading to cancer cell death.

It is well known that CPT and its derivatives also induced an increase of ROS production in various cancer cells, including lung cancer (Brea-Calvo et al. 2009) and breast cancer (Timur et al. 2005). Besides, quinone-containing compounds was showed to activate ERK signaling through upregulating ROS. For instance, benzoquinone was reported to activate ERK/MAPK pathway by modulating the production of ROS in human leukemia HL-60 cells (Ruiz-Ramos et al. 2005). Next, we examined the synergistic effect of TFPP and CPT cotreatment on the ROS production of NSCLC cells. In this study, we found that TFPP cotreatment increased CPT-induced ROS production from 16.3 ± 1.4 to 28.5 ± 0.76 % for A549 and 14.0 ± 0.6 to 23.29 ± 2.7 % for H1299, respectively (Fig. 4). Furthermore, we also showed that the treatment NAC, an ROS scavenger, significantly attenuates ROS production in both A549 and H1299 cells following CPT and TFPP cotreatment (Fig. 5). Furthermore, the MitoSox fluorescence assay confirmed a major source of ROS release from mitochondria by treating CPT alone in NSCLC cells (Supplementary Fig. 2). Besides, NAC pretreatment also decreases CPT and TFPP cotreatment-induced apoptosis in both A549 and H1299 cells (Fig. 6).

On the contrary, MAPK members, including ERK, p38, and JNK, are ROS-induced signal pathways which are involved in survival, proliferation, and death of cells. JNK and p38 are majorly activated by various stresses (Coulthard et al. 2009; Michaelidis et al. 2009). The activation of p38 induces apoptosis by the down-regulation of pro-survival Bcl-2 proteins in response of cellular stress, such as

ROS (Chen et al. 2015) and starvation (Wei et al. 2015). Unlike JNK and p38, ERK mainly regulates growth and survival of cells (McCubrey et al. 2007; Shatos et al. 2008). The constitutive activation and overexpression of ERK were observed in various cancer cell lines, including NSCLC cells (Dhillon et al. 2007; Yamakawa et al. 2016). In addition, the activation of ERK was reported to play an essential role in doxorubicin-chemoresistant breast cancer cells (Smith et al. 2006). In contrast, the blockade of ERK was shown to sensitize cancer cells toward chemotherapy (Abrams et al. 2010). For example, Cho et al. (2009) found that the ERK inhibitor PD98059 significantly enhances tetrandrine, a bis-benzylisoquinoline alkaloid-induced apoptosis of NSCLC A549 cells. This above study suggested that the ERK activation is associated with the pro-survival role.

In this study, we investigated the effect of CPT and TFPP cotreatment on apoptosis of NSCLC cells through downregulating ERK signaling. Our results demonstrate that the both of the phosphorylation sites Thr^{202} and Tyr^{204} of ERK were decreased in TFPP/CPT-cotreated NSCLC cells (Fig. 7a). Although sub-apoptotic-inducing dose (0.5 μM) of CPT causes a significantly increased level of ERK phosphorylation, the Annexin-V-staining assay showed that blockage of ERK partially increases CPT-induced apoptosis of both A549 and H1299 cells (Supplementary Fig. 3), suggesting the pro-survival role of ERK in CPT-treated NSCLC cells.

The members of Bcl-2 family are critical regulators of cellular survival and apoptosis (Cory and Adams 2002; Strasser 2005). Among Bcl-2 proteins, the pro-apoptotic Bim (Bcl-2 interacting mediator of cell death), a BH3-domain only protein, exists as three splicing variants, BimS, BimL and BimEL. Among Bim variants, BimEL prevents that the binding of anti-apoptotic Mcl-1 to Bax/Bak dimer by direct interaction, therefore, facilitates the pro-apoptotic effect of Bax/Bak. BimS induces the apoptosis signaling by directly interacting with Bax, another pro-apoptotic Bcl-2 member (Ewings et al. 2007). In addition, studies showed that the ectopic expression of BimS enhances the thymidine kinase-mediated cell death of malignant glioma cells (Yamaguchi et al. 2003). In contrast, activated ERK could antagonize BimEL-mediate apoptosis by preventing the binding of Bim to pro-survival Bcl-2.

The results of Western blot reveal that TFPP enhances the induction of pro-apoptotic Bim and the proteolytic activation of caspase-9 and -3 by CPT/TFPP combination (Fig. 7a). On the contrary, we also used two caspase inhibitors (death receptor- and mitochondria-mediated caspase cascade) to further determine the apoptosis pathways induced by CPT and TFPP combination, and the blockage of caspase-9 but not caspase-8 largely reduces the apoptosis of both A549 and H1299 cells (Fig. 7b). Furthermore, the blockage of ERK increases the apoptotic population of both A549 and H1299 cells induced by CPT and TFPP cotreatment (Fig. 8). The above results confirmed that the pro-survival role of ERK, and ERK activation may contribute to CPT resistance of NSCLC cells. Taken together, our results suggest that TFPP may sensitize NSCLC cells towards CPT treatment via upregulating endogenous ROS, the suppression of ERK, and the increase of Bim variants BimL and BimS, eventually lowering the threshold of apoptosis.

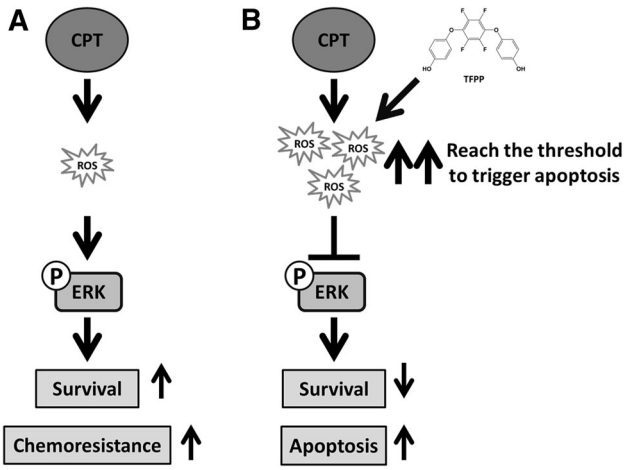

Fig. 9 Potential mechanism underlying the synergistic effect of TFPP on CPT-induced apoptosis of both A549 and H1299 cells through regulating ROS generation and ERK. **a** When CPT treatment alone, the increased level of CPT-induced ROS is not sufficient to inhibit cellular proliferation and induce apoptosis of NSCLC cells. Instead, the activation of ERK induced by CPT may contribute to cell survival and the acquired chemoresistance of NSCLC. **b** When cotreatment of CPT and TFPP, the endogenous ROS is dramatically accumulation and this may cause a reduction of apoptosis threshold-induced by ROS. Furthermore, the high level of endogenous ROS induced by CPT and TFPP cotreatment also inhibits ERK activation, upregulating the expression of prop-apoptotic protein Bim, eventually sensitizes NSCLC cells to CPT, and enhances the apoptotic population of NSCLC cells

In conclusion, in this study, we demonstrate the synergistic effect of TFPP on CPT-induced apoptosis of human lung cancer cells. The cotreatment of TFPP and CPT increases the endogenous ROS and suppresses the activation of pro-survival ERK, lowering the threshold of apoptosis in lung cancer cells (Fig. 9). Accordingly, TFPP may be a promising chemosensitizer to CPT-based therapies, such as irinotecan or topotecan, and this should benefit to treat those lung cancer cells which are insensitive to CPT or other ROS-inducing anti-neoplastic compounds.

Acknowledgments This study was supported by the Grants #MOST101-2320-B-037-046-MY3 and #MOST 102-2632-B-037-001-MY3 from the Ministry of Science and Technology (MOST), Taiwan; by the Grant #KMU-TP104A03 from the KMU Research

Project, Taiwan; by the Grant #NSYSUKMU104-P031 from the NSYSU-KMU Joint Research Project, Taiwan; and by the Grant #104-CM-KMU-006 from ChiMei-KMU Joint Research Project, Taiwan. We are also grateful for the instrument supports of flow cytometry from the Center for Research Resources and Development at Kaohsiung Medical University, Taiwan.

References

Abrams SL, Steelman LS, Shelton JG et al (2010) The raf/mek/erk pathway can govern drug resistance, apoptosis and sensitivity to targeted therapy. Cell Cycle 9:1781–1791

Barrera G (2012) Oxidative stress and lipid peroxidation products in cancer progression and therapy. ISRN Oncol 2012:137289

Benites J, Valderrama JA, Rivera F et al (2008) Studies on quinones. Part 42: synthesis of furylquinone and hydroquinones with antiproliferative activity against human tumor cell lines. Bioorg Med Chem 16:862–868

Bolton JL, Trush MA, Penning TM et al (2000) Role of quinones in toxicology. Chem Res Toxicol 13:135–160

Brea-Calvo G, Siendones E, Sanchez-Alcazar JA et al (2009) Cell survival from chemotherapy depends on NF-kappaB transcriptional up-regulation of coenzyme q biosynthesis. PLoS One 4:e5301

Chen K, Chu BZ, Liu F et al (2015) New benzimidazole acridine derivative induces human colon cancer cell apoptosis in vitro via the ROS-JNK signaling pathway. Acta Pharmacol Sin 36:1074–1084

Chiu CC, Chou HL, Chen BH et al (2015) Bpiq, a novel synthetic quinoline derivative, inhibits growth and induces mitochondrial apoptosis of lung cancer cells in vitro and in zebrafish xenograft model. BMC Cancer 15:962

Cho HS, Chang SH, Chung YS et al (2009) Synergistic effect of erk inhibition on tetrandrine-induced apoptosis in a549 human lung carcinoma cells. J Vet Sci 10:23–28

Chou TC, Talalay P (1981) Generalized equations for the analysis of inhibitions of michaelis-menten and higher-order kinetic systems with two or more mutually exclusive and nonexclusive inhibitors. Eur J Biochem 115:207–216

Chou TC, Talalay P (1984) Quantitative analysis of dose-effect relationships: the combined effects of multiple drugs or enzyme inhibitors. Adv Enzyme Regul 22:27–55

Cimino GD, Pan CX, Henderson PT (2013) Personalized medicine for targeted and platinum-based chemotherapy of lung and bladder cancer. Bioanalysis 5:369–391

Cory S, Adams JM (2002) The BCL2 family: regulators of the cellular life-or-death switch. Nat Rev Cancer 2:647–656

Coulthard LR, White DE, Jones DL et al (2009) P38(MAPK): stress responses from molecular mechanisms to therapeutics. Trends Mol Med 15:369–379

Dhillon AS, Hagan S, Rath O et al (2007) MAP kinase signalling pathways in cancer. Oncogene 26:3279–3290

Ewings KE, Wiggins CM, Cook SJ (2007) Bim and the pro-survival BCL-2 proteins: opposites attract, ERK repels. Cell Cycle 6:2236–2240

Fong Y, Lin YC, Wu CY et al (2014) The antiproliferative and apoptotic effects of sirtinol, a sirtuin inhibitor on human lung cancer cells by modulating AKT/beta-catenin-FOXO3a axis. Sci World J 2014:937051

Fraser M, Leung B, Jahani-Asl A et al (2003) Chemoresistance in human ovarian cancer: the role of apoptotic regulators. Reprod Biol Endocrinol 1:66

Gallego MA, Ballot C, Kluza J et al (2008) Overcoming chemoresistance of non-small cell lung carcinoma through restoration of an aif-dependent apoptotic pathway. Oncogene 27:1981–1992

Hung JJ, Jeng WJ, Hsu WH et al (2012) Predictors of death, local recurrence, and distant metastasis in completely resected pathological stage-I non-small-cell lung cancer. J Thorac Oncol 7:1115–1123

Ichinose Y, Seto T, Nishiwaki Y et al (2011) Phase I study of topotecan and cisplatin in patients with small cell lung cancer. Jpn J Clin Oncol 41:197–203

Jayasooriya RG, Choi YH, Hyun JW et al (2014) Camptothecin sensitizes human hepatoma HEP3b cells to trail-mediated apoptosis via ROS-dependent death receptor 5 upregulation with the involvement of MAPKs. Environ Toxicol Pharmacol 38:959–967

Kim HT, Han JY, Lee DH et al (2006) A phase II study of irinotecan plus cisplatin for patients with advanced stage IIIB or IV NSCLC previously treated with nonplatinum-based chemotherapy. Cancer 107:799–805

Liang Y, Wakelee HA (2013) Adjuvant chemotherapy of completely resected early stage non-small cell lung cancer (NSCLC). Transl Lung Cancer Res 2:403–410

McCubrey JA, Steelman LS, Chappell WH et al (2007) Roles of the raf/mek/erk pathway in cell growth, malignant transformation and drug resistance. Biochim Biophys Acta 1773:1263–1284

Michaelidis B, Hatzikamari M, Antoniou V et al (2009) Stress activated protein kinases, JNKs and p38 MAPK, are differentially activated in ganglia and heart of land snail helix lucorum (l.) during seasonal hibernation and arousal. Comp Biochem Physiol A: Mol Integr Physiol 153:149–153

Mor G, Montagna MK, Alvero AB (2008) Modulation of apoptosis to reverse chemoresistance. Methods Mol Biol 414:1–12

Ogawa K, Hosokawa A, Ueda A et al (2012) Irinotecan plus mitomycin c as second-line chemotherapy for advanced gastric cancer resistant to fluoropyrimidine and cisplatin: a retrospective study. Gastroenterol Res Pract 2012:640401

Okon IS, Coughlan KA, Zhang M et al (2015) Gefitinib-mediated reactive oxygen specie (ROS) instigates mitochondrial dysfunction and drug resistance in lung cancer cells. J Biol Chem 290:9101–9110

Ong JY, Yong PV, Lim YM et al (2015) 2-Methoxy-1,4-naphthoquinone (MNQ) induces apoptosis of a549 lung adenocarcinoma cells via oxidation-triggered JNK and p38 MAPK signaling pathways. Life Sci 135:158–164

Patankar NA, Pritchard J, van Grinsven M et al (2013) Topotecan and doxorubicin combination to treat recurrent ovarian cancer: the influence of drug exposure time and delivery systems to achieve optimum therapeutic activity. Clin Cancer Res 19:865–877

Patel SH, Ajlouni M, Chapman R et al (2007) A prospective phase ii study of induction carboplatin and vinorelbine followed by concomitant topotecan and accelerated radiotherapy (ART) in locally advanced non-small cell lung cancer (NSCLC). J Thorac Oncol 2:831–837

Read W, McLeod H, Govindan R (2004) Irinotecan and carboplatin in metastatic or recurrent NSCLC: an update. Oncology 18(14 Suppl 14):15–17

Ruiz-Ramos R, Cebrian ME, Garrido E (2005) Benzoquinone activates the erk/mapk signaling pathway via ROS production in HL-60 cells. Toxicology 209:279–287

Sharma V, Joseph C, Ghosh S et al (2007) Kaempferol induces apoptosis in glioblastoma cells through oxidative stress. Mol Cancer Ther 6:2544–2553

Shatos MA, Gu J, Hodges RR et al (2008) Erk/p44p42 mitogen-activated protein kinase mediates egf-stimulated proliferation of conjunctival goblet cells in culture. Invest Ophthalmol Vis Sci 49:3351–3359

Shi K, Wang D, Cao X et al (2013) Endoplasmic reticulum stress signaling is involved in mitomycin C (MMC)-induced apoptosis in human fibroblasts via perk pathway. PLoS One 8:e59330

Smith L, Watson MB, O'Kane SL et al (2006) The analysis of doxorubicin resistance in human breast cancer cells using antibody microarrays. Mol Cancer Ther 5:2115–2120

Strasser A (2005) The role of BH3-only proteins in the immune system. Nat Rev Immunol 5:189–200

Strauss GM, Herndon JE 2nd, Maddaus MA et al (2008) Adjuvant paclitaxel plus carboplatin compared with observation in stage IB non-small-cell lung cancer: CALGB 9633 with the cancer and leukemia group b, radiation therapy oncology group, and north central cancer treatment group study groups. J Clin Oncol 26:5043–5051

Tait SW, Green DR (2010) Mitochondria and cell death: outer membrane permeabilization and beyond. Nat Rev Mol Cell Biol 11:621–632

Tamburini M, Buccheri G, Brunelli C et al (2000) The difficult choice of chemotherapy in patients with unresectable non-small-cell lung cancer. Support Care Cancer 8:223–228

Timur M, Akbas SH, Ozben T (2005) The effect of topotecan on oxidative stress in MCF-7 human breast cancer cell line. Acta Biochim Pol 52:897–902

Trachootham D, Lu W, Ogasawara MA et al (2008) Redox regulation of cell survival. Antioxid Redox Signal 10:1343–1374

Trachootham D, Alexandre J, Huang P (2009) Targeting cancer cells by ROS-mediated mechanisms: a radical therapeutic approach? Nat Rev Drug Discov 8:579–591

Tsang WP, Chau SP, Kong SK et al (2003) Reactive oxygen species mediate doxorubicin induced p53-independent apoptosis. Life Sci 73:2047–2058

Uramoto H, Tanaka F (2014) Recurrence after surgery in patients with NSCLC. Transl Lung Cancer Res 3:242–249

Wang J, Yi J (2008) Cancer cell killing via ROS: to increase or decrease, that is the question. Cancer Biol Ther 7:1875–1884

Wang J, Yuan Z (2013) Gambogic acid sensitizes ovarian cancer cells to doxorubicin through ROS-mediated apoptosis. Cell Biochem Biophys 67:199–206

Wang CY, Cusack JC Jr, Liu R et al (1999) Control of inducible chemoresistance: enhanced anti-tumor therapy through increased apoptosis by inhibition of NF-kappaB. Nat Med 5:412–417

Wei Y, An Z, Zou Z et al (2015) The stress-responsive kinases MAPKAPK2/MAPKAPK3 activate starvation-induced autophagy through beclin 1 phosphorylation. Elife 4:e05289

Westover D, Ling X, Lam H et al (2015) Fl118, a novel camptothecin derivative, is insensitive to ABCG2 expression and shows improved efficacy in comparison with irinotecan in colon and lung cancer models with ABCG2-induced resistance. Mol Cancer 14:92

Wirth M, Berthold E, Grashoff M et al (1994) Detection of mycoplasma contaminations by the polymerase chain reaction. Cytotechnology 16:67–77

Xenidis N, Vardakis N, Varthalitis I et al (2011) Alpha multicenter phase ii study of pegylated liposomal doxorubicin in combination with irinotecan as second-line treatment of patients with refractory small-cell lung cancer. Cancer Chemother Pharmacol 68:63–68

Yamaguchi T, Okada T, Takeuchi K et al (2003) Enhancement of thymidine kinase-mediated killing of malignant glioma by BIMS, a BH3-only cell death activator. Gene Ther 10:375–385

Yamakawa K, Yokohira M, Nakano Y et al (2016) Activation of MEK1/2-ERK1/2 signaling during NNK-induced lung carcinogenesis in female A/J mice. Cancer Med 5:903–913

Yang XQ, Li CY, Xu MF et al (2015) Comparison of first-line chemotherapy based on irinotecan or other drugs to treat non-small cell lung cancer in stage IIIB/IV: a systematic review and meta-analysis. BMC Cancer 15:949

Zeng CW, Zhang XJ, Lin KY et al (2012) Camptothecin induces apoptosis in cancer cells via microrna-125b-mediated mitochondrial pathways. Mol Pharmacol 81:78–586